Deep Learning Approach for Non-destructive Radiography Testing of Piping Welds

Adil EL HARRAK, Mohamed RHAZZAF, *Member, IAENG,* and Imane MOUMENE.

Abstract—**Radiographic testing is the most common method of non-destructive testing to detect discontinuities in industrial piping welds. Human interpretation of radiographic films is time-consuming and requires high degrees of expertise. Despite the significant advancements of deep learning techniques in related fields, such as medical radiography, prior research endeavors focused on weld discontinuities were constrained by the limitations stemming from a lack of training data and their inadequate representation of real-world conditions in the field.**

This paper introduces a comprehensive system that automatically detects welding zones, assesses film quality, and classifies weld discontinuities for the piping process. The proposed framework demonstrates superior generalization capabilities that bypass a single industry or piping size. The key advantages of our technique lie in its enhanced accuracy, rapid processing, and automatic interpretation of welding films across a wide range of image qualities. Consequently, it achieves remarkable detection and classification accuracy, offering substantial benefits for welding inspection and quality assessment.

Index Terms—**Deep Learning, image processing, Quality Control, Welding, Process Piping, Conventional Radiography, Weld defects, Non-destructive Testing, Digital Radiography**

I. INTRODUCTION

Process pipes are the main components of most industrial facilities. The global production of those products was 86 million tons in 2018 and could exceed 109 million tons in 2023 [1]. According to a recent report, the market size of process piping reaches 277 million USD, owing to the growing demand from end-use industries [1]. Non-destructive testing (NDT) of process piping ensures safe and productive operations in critical applications. Specifically, companies commonly use radiography for quality control in oil, gas, chemical, and other piping systems. Typically, certified NDT inspectors interpret gamma-ray radiographs following international standards. This task is time-consuming, especially before plant commissioning, which involves thousands of radiographs. Weld discontinuities are subtle and small. Hence, the process involves multiple levels of verification to ensure quality assurance.

Machine learning techniques offer compelling opportunities for the automatic detection of flaw indications. Artificial intelligence methods give successful results for interpreting medical imagery with accuracy akin to human experts [2], [3]. New advancements in artificial intelligence in image processing drive industrial application markets. In fact, according to market studies, the expected market size of image recognition will grow from 26 million USD in 2020 to exceed 50 million in 2025 [4].

Previous research handled welding discontinuity detection challenges with image processing techniques and neural networks [5]. However, image processing lacks the ability for generalization. The downside of this method is that it requires determining which aspects of each image are essential. Moreover, the feature extraction process becomes more difficult as the number of classes to categorize grows [6].

Using neural networks for weld radiographs seems promising. Hence, different attempts were conducted to develop an automatic way to detect welding discontinuities [7], [8], [9]. Previous studies tackled welding discontinuity classification with limitations caused by many issues, like the size and the misrepresentation of data, as well as the lack of diversity in discontinuity type. Most recent studies focus on digital radiography because images are more abundant and have higher image quality and resolution. Indeed, conventional radiography remains the most used non-destructive testing method in the process industries, including the main application of pipe welding control. Even if many authors have conducted many studies, the problem is still insufficiently explored. [8] proposed an approach for resolving the digital weld radiograph classification using convolutional neural networks. The system achieved significant accuracy for large diameters from a single industrial plant and was constrained to high image resolution achievable solely with digital radiography.

We have organized the rest of this paper as follows: Section 2 introduces process piping fabrication and quality control using radiography testing. Section 3 extends the overview of the past studies related to our subject. Section 4 presents the model architecture, the learning procedures, and the dataset. Section 5 will highlight the simulation and results. Section 7 summarizes the main findings and provides concluding remarks, including possible directions for further research.

II. PROCESS PIPING

One of the crucial systems in the processing and exploration industries is process piping. ”Process piping” generally refers to a system that transports process fluids like air, water, steam, and gaseous and liquid hydrocarbons

Manuscript received Apr 12, 2023; revised Jan 23, 2024. This work was supported in part by Moulay Ismail University, Meknes, Morocco.

Adil El Harrak is a Mechanical and Structures engineer and an International Welding Technologist. ENSAM-Moulay Ismail University Meknes, Morocco. e-mail: a.elharrak1@gmail.com.

Mohamed Rhazzaf is an assistant professor and researcher in computer science and artificial intelligence, Artificial Intelligence and Applications laboratory (AIA), Euro-Med Research Center, Euro-Med University. Fez, Morocco e-mail: m.rhazzaf@edu.umi.ac.ma.

Imane Moumene an industrial and production engineer Inspection (NDT & Lifting) manager ENSAM-Meknes, Moulay Ismail University, Meknes, Morocco e-mail: moumeneimane@gmail.com.

around an industrial installation under pressure or vacuum.

As defined by ASME B31.3 [10], process piping is the piping that conveys fluids under pressure or vacuum within the limits of a petroleum refinery, chemical plant, gas processing plant, pharmaceutical, textile, paper, semiconductor, cryogenic, and related processing plants and terminals. The American Society of Mechanical Engineers (ASME) B31.3 Codes are considered the ultimate international standard for piping in processing plants and industrial installations. Canada also assigns this code, as it is a requirement in the U.S. according to the Occupational Safety and Health Administration (OSHA) for all process piping, and many industrial insurance carriers further mandate industrial facilities [11].

Process piping systems provide various industrial and manufacturing functions, such as liquid mixing, separating, stopping, starting fluid flow, pressurization, depressurization, and filtering.

A. Process piping fabrication

Generally, various materials make up process piping, including steel, alloy steel, stainless steel, glass-reinforced plastic, or specific materials in particular use cases. The described complex systems are typically composed of a prefabricated single-pipe spool. Pipe spool fabrication is an influential stage of process piping. It is a production system characterized by mixed components like pipes, flanges, and fittings assembled generally by welding. In the outlet extremity of pipe spools, often control instruments are built by threading. Finally, valves, bolts, nuts, and gaskets connect those pipe spools. We can include other components to facilitate mixing, separating, pressurizing, or other functions. The exact makeup of a process piping system will depend entirely on the application the system serves.

Process piping is the safest tool to transport fluids and gases across platforms or manufacturing facilities. However, piping failure may cause damage to human workers and industrial facilities. Often, investigating such failures involves input from various engineering disciplines, particularly welding, non-destructive testing, and fracture mechanics. Given the potential consequences of weld piping failures, mitigating failure risk is critical. Experts provide in-depth technical knowledge that helps to detect welding defects efficiently by recommending the proper control procedure that frequently incorporates gamma-ray radiography.

B. Quality control of process piping systems

Pipe spool fabrication is one of the most complex industrial processes. The primary purpose of process piping is to manufacture pipe spools, which refer to a section of a piping system prefabricated as smaller segments with flanges and fittings. The typical operations of pipe spool manufacturing include cutting, fitting, welding, post-weld heat treatment, and coating.

Industrially, all piping activities are performed in compliance with the international and industrial codes and standards, as well as the laws and regulations of the respective local authorities. There are three stages of quality control (QC) for prefabricated pipe spools:

- Before welding, we cut the raw pipes to the required size. Then, they are fitted for welding. QC in this stage consists of 100% visual control to detect imperfections on edges to be welded and ensure compliance and quality of assembly preparation.
- During welding, the objective of quality control is to ensure the conformity of welding between passes, verify the nature and size of filler metal, control the voltage and amperage of the welding machine, and verify welding speed.
- Quality control of prefabricated pipe spools after welding is generally an application of non-destructive testing (NDT) in welded joints and mechanical testing by the hydraulic test of pressure about 1.5 of the rating flange.

NDT is used to verify the conformity of welds. There is a difference between discontinuity, defect, and indication. As defined by the ASME V code, a discontinuity is a lack of continuity or cohesion, an intentional or unintentional interruption in the physical structure or configuration of a material or component. An indication is a response or evidence from a non-destructive examination that requires interpretation to determine relevance. Moreover, a defect is one or more flaws whose aggregate size, shape, orientation, location, or properties do not meet specified acceptance criteria and are rejectable [12].

The non-destructive inspection aims to determine if the inspected entity is to be accepted or rejected. The inspector looks for discontinuities in the object and identifies their nature and size. Then, those discontinuities are evaluated according to acceptance criteria and determined as defects or not. For an easy evaluation, we regroup the indications into two categories [12]:

- A linear indication represents any indication with a length greater than three times the width. Linear indications are mainly cracks, lack of penetration, lack of fusion, and elongated slag inclusions.
- A rounded indication signifies any indication with a length equal to or less than three times the width, like porosity and tungsten inclusion.

Various NDT methods are used to evaluate the quality of welds. Radiographic testing is the most common non-destructive testing method used to detect discontinuities. The process can perform well in the internal structure of weld joints in prefabricated pipe spools.

C. Radiography testing

As a tool used in various applications, including medicine and industrial plants, radiographic testing is one of the primary non-destructive testing (NDT) methods to

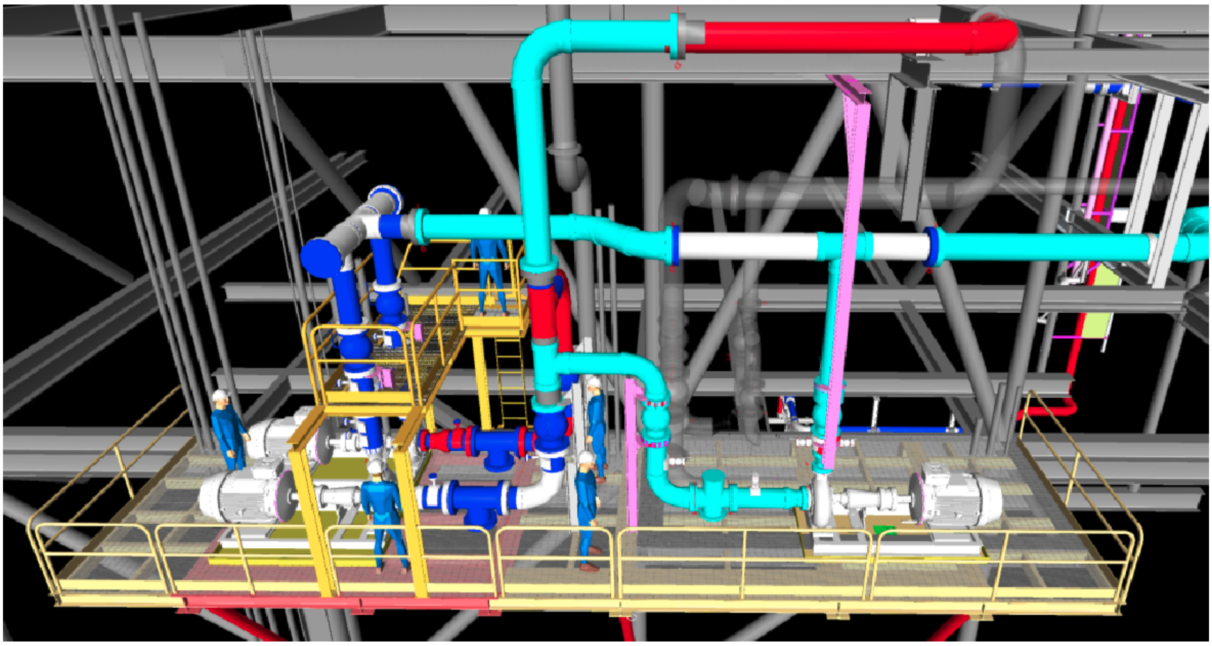

Fig. 1: Complex industrial piping system of a hydrocyclone skid in an offshore petroleum platform (source: IIS with permission)

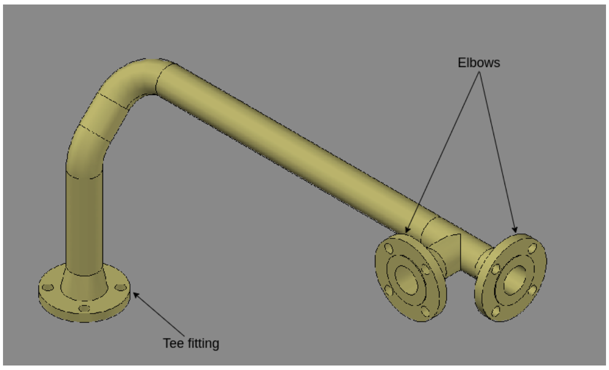

Fig. 2: Example of a welded pipe spool containing three flanges, a Tee fitting, and two elbows (source: IIS with permission)

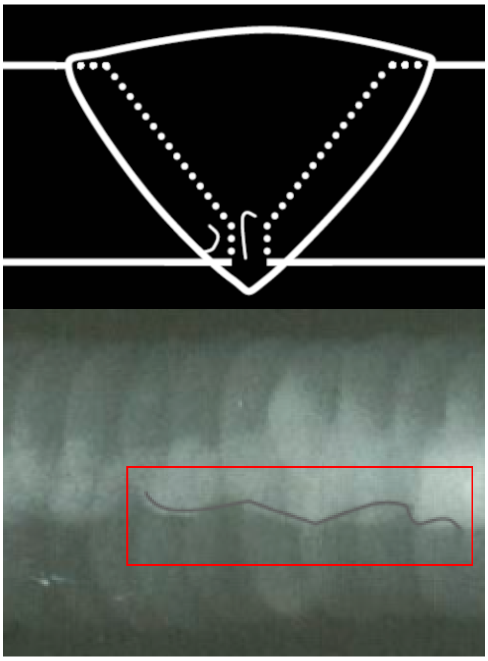

Fig. 3: Symbol and real photo of crack

detect discontinuities. Radiography testing is one of the NDT methods that uses either gamma rays produced by radioactive isotopes or electrically generated x-rays to detect the presence of internal material discontinuities [12].

As shown in figure 9, gamma rays pass through the tested weld into a photographic film, resulting in an image of the internal material. The tested joint is placed between the radiation source and the detector. The studied material density and thickness differences attenuate the penetrating radiation through interaction processes that include scattering, absorption, or both. We use the image darkness variation to determine the thickness or composition of the material. It would also reveal the presence of any flaws or discontinuities inside the material.

The radiation source can either be an X-ray machine or a radioactive source (Ir-192, Co-60, or, in rare cases, Cs-137). The joints of assembled parts will stop some radiation, whereas thicker and denser areas will stop more radiation. The radiation that passes through the welded joint will expose the film, forming a shadow of the weld. The film's darkness or density will vary with the amount of radiation reaching the film through the test object, where darker areas indicate more exposure (higher radiation intensity) and lighter areas indicate less exposure (lower radiation intensity).

Radiography testing is suitable for inspecting hidden flaws using short-wavelength electromagnetic radiation (high-energy photons) to penetrate various materials. The radiation intensity that penetrates and passes through the material is either captured by a radiation-sensitive film (conventional

TABLE I: Different assembly joint types

Assembly joint type	3D View	2D View	Isometrical symbol	Assembly elements
Flange butt welding neck to pipe	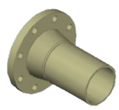	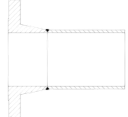		Flange + Pipe
Flange socket weld to pipe	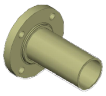	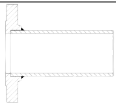	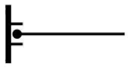	Flange + Pipe
Weldolet in pipe	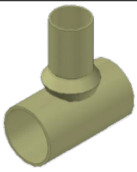	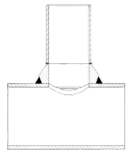	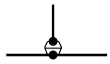	Weldolet + Pipe
Pipe to Elbow butt weld		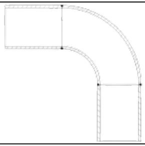		Pipe + Elbow
Tee butt weld to pipe	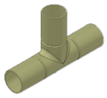	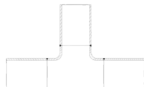	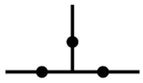	Tee + Pipe
Flange slip on to pipe	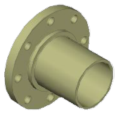	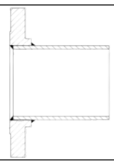	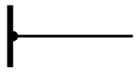	Flange + Pipe

TABLE II: Discontinuity type description

discontinuity type	Symbol in labeling	Description
Crack	**FU**	Imperfection produced by a fracture that can arise from the stresses generated most of the time during cooling. It is known as hydrogen introduction in surface or subsurface welding areas. It is the most serious defect found in a weld and should be removed.
Lack of fusion or incomplete fusion	**MF**	A weld discontinuity in which fusion does not occur between weld metal and fusion faces or adjoining weld beads. It is the failure of the filler metal to fuse with the adjacent base metal because the surface of the base metal did not reach melting temperature during welding.
Porosity	**S**	Small cavities or bores, which mostly have a spherical shape. Porosity occurs when some constituents of the molten metal vaporize, causing small gas pockets that get entrapped in the metal as it solidifies. These small bores could have a variety of shapes, but mostly they have a spherical shape.
Cluster porosity	**NS**	Regular porosity in the radiograph, but as a closed cluster group. In general, the cause of the cluster of porosity is when flux-coated electrodes are contaminated with moisture. The moisture becomes a gas when heated and trapped in the weld during the welding process.
Slag inclusions	**IL**	Mostly happens in shielded metal arc welding (SMAW), and it occurs when the slag cannot float to the surface of the molten metal and gets entrapped in the weld metal during solidification.
Tungsten inclusions	**IT**	This type of inclusion can be found in weld metal deposited by gas tungsten arc welding (GTAW) as a result of allowing the tungsten electrode to come into contact with the molten metal.

radiography) or a planar array of radiation-sensitive sensors (digital radiography). Conventional radiography is the oldest approach, yet it is still the most widely used in NDT, especially for pipe welds, given the limitations of digital radiography testing in terms of diameter and thickness.

The Image Quality Indicator (IQI) or ”Penetrameter” is used as a test piece in radiography testing to establish and control the film image quality. It is placed on the test object and radiographed to evaluate the radiograph’s sensitivity. The IQI consists of wires of varying thicknesses and holes.

Numerous radiographic techniques are utilized in non-destructive testing processes, with the most common ones being the Single Wall Single Image (SWSI), the Double Wall Double Image (DWDI), and the Double Wall Single Image (DWSI)..

The Single Wall Single Image is employed when the interior of a pipe is readily accessible. In this technique, the radiation source is positioned on one side, with the film placed in close proximity on the opposite side.

The Double Wall Double Image technique involves the passage of radiation through two walls, capturing the material or weld on the same radiograph. In the case of welds, the radiation beam may be strategically offset from the weld plane at an adequate angle to separate the source-side images and film-side segments, preventing overlap in interpreted areas. In the Double Wall Single Image methodology, the radiation traverses through two walls. However, only the material or weld in close proximity to the film side is visible to achieve an optimal exposure number and guarantee the requisite coverage.

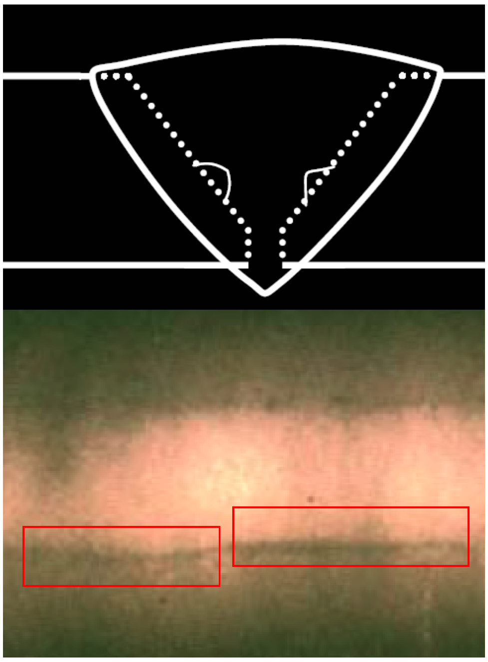

Fig. 4: Symbol and real photo of lack of fusion or incomplete fusion

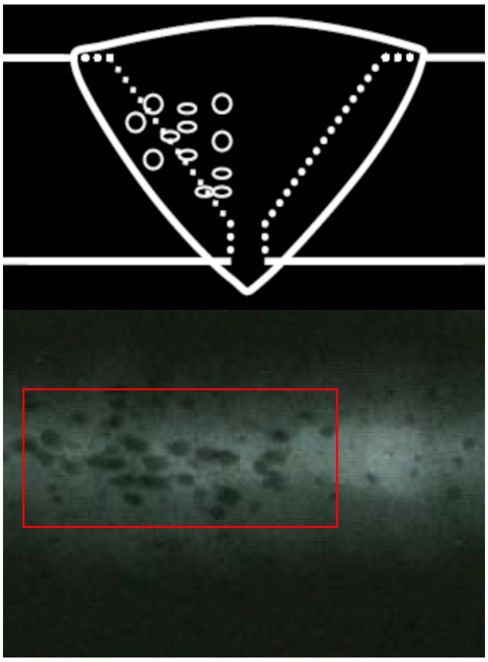

Fig. 6: Symbol and real photo of cluster porosity

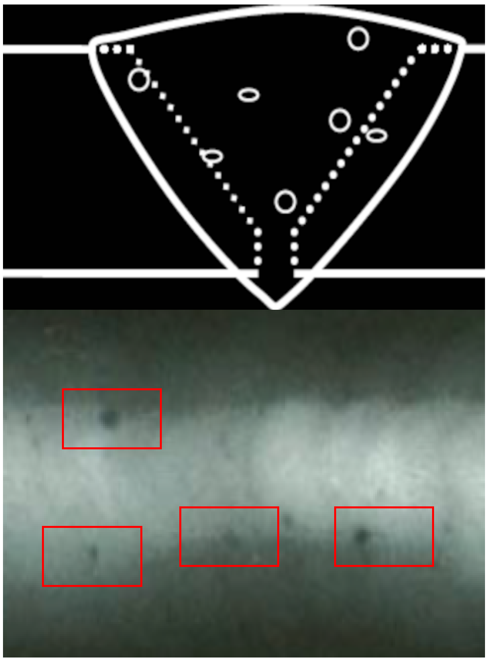

Fig. 5: Symbol and real photo of porosity

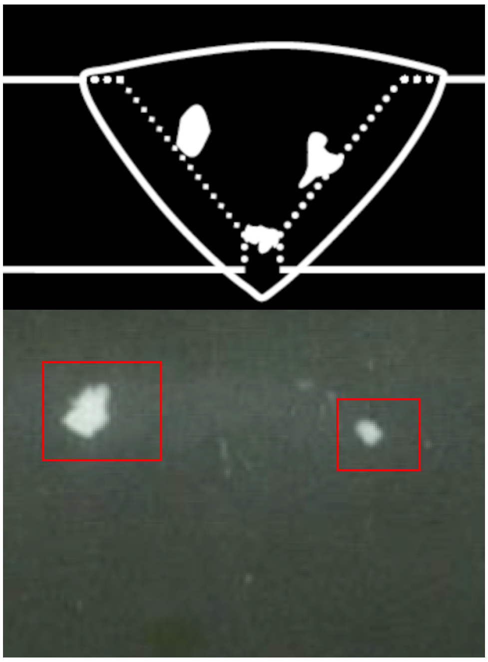

Fig. 7: Symbol and real photo of slag inclusions

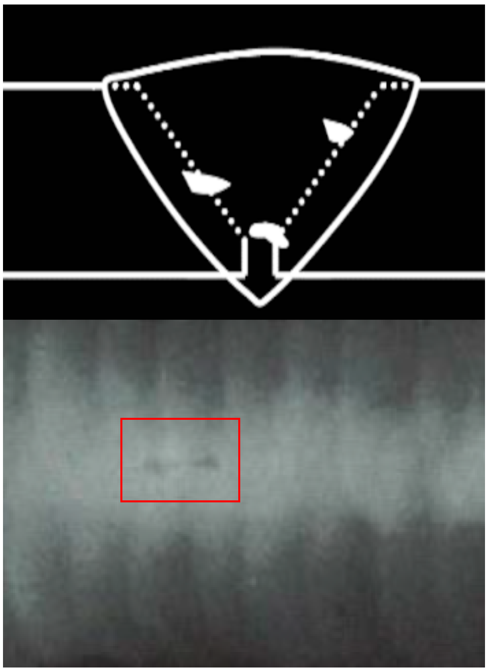

Fig. 8: Symbol and real photo of tungsten inclusions

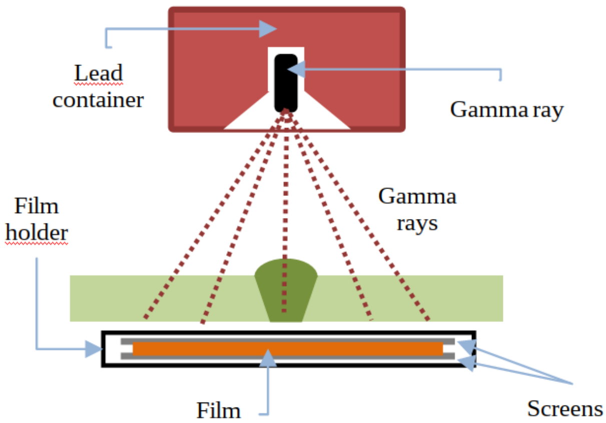

Fig. 9: Principles of gamma-ray shooting apparatus

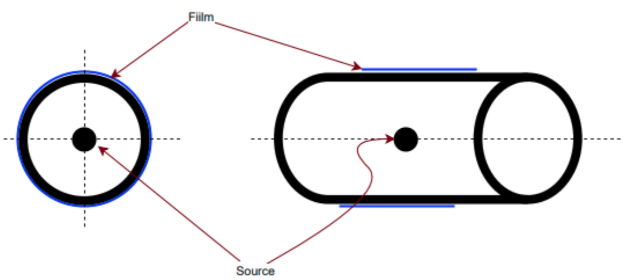

Fig. 10: Single Wall Single Image (SWSI)

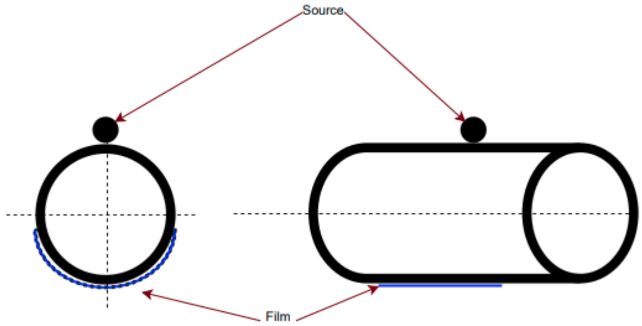

Fig. 11: Double Wall Double Image (DWDI)

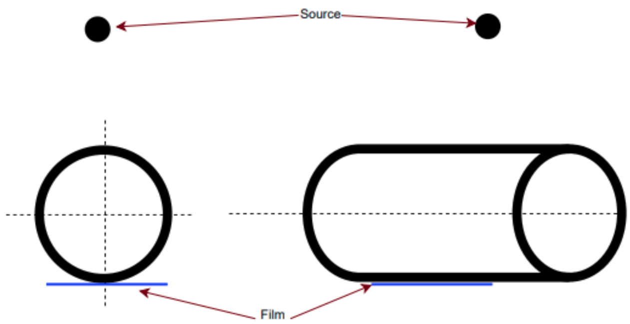

Fig. 12: Double Wall Single Image (DWSI)

III. Image processing for weld discontinuities

Weld discontinuities are a geometrical feature extraction problem, so the first effort is to use image processing and a geometric extraction algorithm. Radiographic images often show low contrast, noise presence, and an uneven distribution of grays. However, the quality of images influences the detection of weld defects to a large extent, especially for those small defects that drown in the noise. So image processing has the purpose of reducing noise and enhancing contrast. Image preprocessing in our context is a critical operation that demands careful consideration. It is essential to highlight that a solution must execute the process with the utmost care to avoid any loss of vital information from the image.

Many papers use methods to remove noise and keep as much vital information related to weld defects as they can. [13] designed a one-dimensional FFT filter for detecting the crack flaw. The filter can distinguish between undercuts and cracks. [14] employs a wavelet filter to minimize the noise with a simple threshold. Many works applied standard filters like the median or adaptive Wiener filter to remove the noise from images [15], [16]. [17] mix an adaptive Wiener filter and a Gaussian low-pass filter to remove noise. The adaptive filter preserves edges and other high-frequency information. At the same time, the Gaussian low-pass filter smooths an image in the frequency domain by alternating a specific range of high-frequency components.

Filtering methods suffer from the tuning configuration, such as the size of the filter and threshold values. In contrast, other methods use machine learning approaches to tackle noise problems. [18] used blind image separation (BIS) instead of filtering. The technique applies transformation and classification machine learning algorithms to separate noise from the information.

Contrast enhancement aims to highlight the geometric features of the image. With the weld defect image's low contrast nature due to the limitation of the intensity range accommodated by the capture device and the presence of noise, such an operation is much needed.

[18] uses contrast stretching and normalization algorithms to enhance images. The idea first normalizes the image with low and high thresholds, finds the values closest to the minimum and maximum values, and performs contrast stretching according to the specific range of contrast values. [19] applies histogram stretching and equalization to get the best image before the segmentation. The histogram stretching algorithm increases the contrast of an image. The goal of histogram equalization is to obtain an image with uniformly distributed brightness levels across the entire range. The sin function enhancement method in [20] improved the contrast of the weld and background regions. After that, the background area's gray and weld areas are concentrated into high and low gray levels, and the curve is double-peaked.

IV. The proposed approach

As discussed before, the main difficulties of welding discontinuity detection reside in two things. The first is keeping useful image information with quality enhancement. The second is related to the tiny and various geometrical discontinuities. Convolutional neural networks have proven themselves in object detection because of their many advantages, such as geometrical feature extraction and local connectivity. Object detection networks are mainly divided into two categories: single-stage and two-stage. Based on a one-step strategy, the model directly regresses the classification and location of objects, which can achieve fast detection speeds and is efficient and hardware-friendly. YOLO [21], SSD [22], RetinaNet [23], VFNet [24], and RepPoints [25] are examples of one-stage convolutional neural networks. Compared to one-stage networks and two-stage methods such as Faster RCNN [26], Cascade R-CNN [27], R-FCN [28], and Dynamic RCNN [29], have low inference speeds because they generate region proposals that distinguish between foreground and background first. However, the refined design improves the recognition performance and is more suitable for the high-precision scene.

To implement the welding discontinuity detection approach from a hardware-friendly perspective In addition, for the welding testing, we use just images. Our approach will target mainly efficient computation goals, in addition to attempting good precision in detection.

A. The proposed model

The proposed model splits the welding discontinuity detection into four stages:

- **The validation of the proposed film**: In this stage, we look for the presence of all elements imposed by one of the international welding standards. In our example, we seek to visualize the welding zone, the norm zone, and at least three characterizing wires.
- **Images cleaning**: To increase the quality of the original welding image, we apply the histogram equalizer image preprocessing to preserve its information. For example, we choose "Contrast Limited Adaptive Histogram Equalization"[30] (CLAHE).
- **Preparation of the welding zones**: including a method for cropping the welding zone into near-square-shaped fragments. This step is necessary for enlarging the discontinuity zone ratio within the fragment's surface. We should mention that getting a comprehensive coordinate of the discontinuity zone within the original first image imposes the attribution of a transition vector for each near square fragment, expressed as (x_f, y_f), where x_f, y_f are respectively the coordinates of the top left corner of each fragment within the original first image top left corner.
- **The detection of discontinuities**: In each near-square welding fragment image, we precede the detection of any discontinuities and use the transition vector to get the final coordinates.

B. Dataset preparation

1) Welding discontinuities type choice : According to the gamma-ray shooting method, the proposed dataset regroups two types of radiograph welds: elliptical shooting for weld

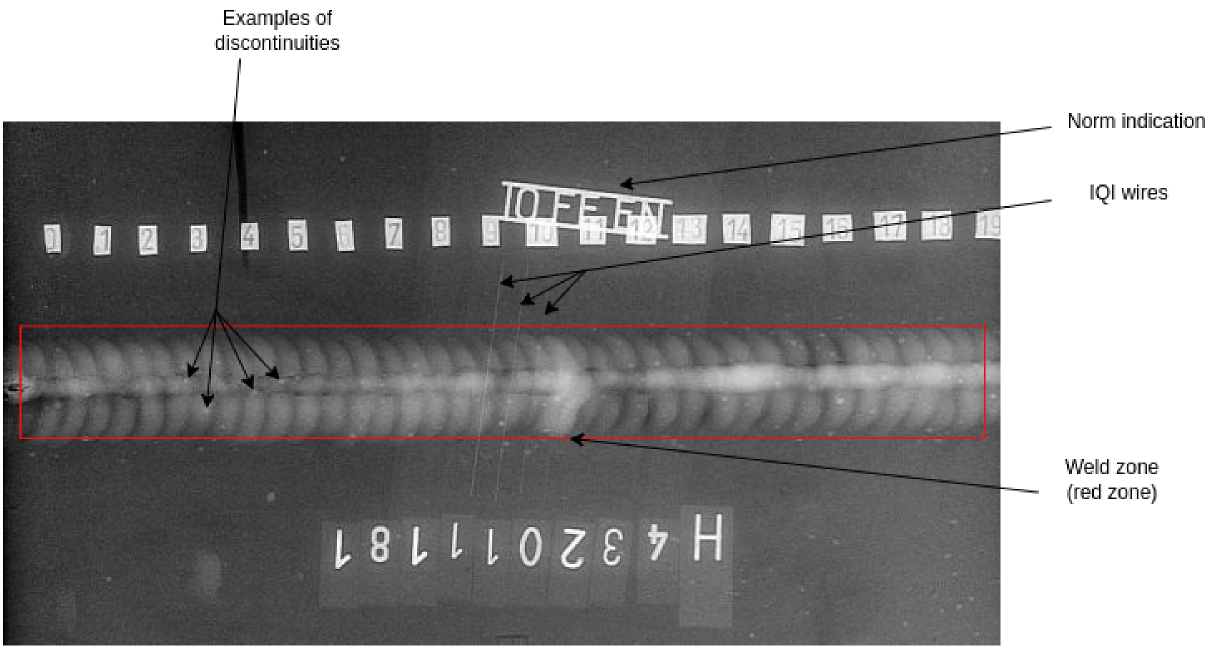

Fig. 13: A radiograph of a tested weld showing the norm, IQI wires, the welding zone, and discontinuities

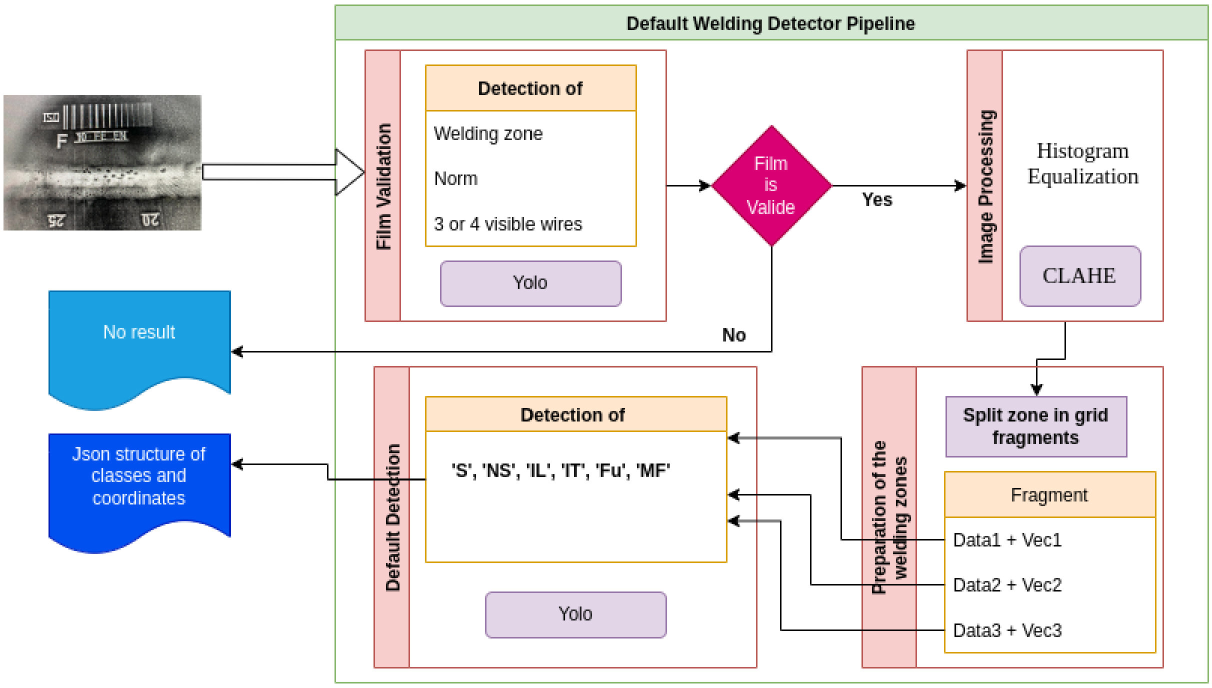

Fig. 14: Model architecture

pipe diameters inferior to 2 inches and shooting contact for weld pipe diameters strictly superior to 2 inches.

The dataset comprises piping weld radiographs ranging in thickness from 3.91 mm (diameter of 0.75 inches) to 17.14 mm (diameter of 12 inches).

The proposed model aims to detect the number of wires as a function of the thickness of the radiographed weld. The model did not take this option as the naked eye quickly detects IQI holes.

2) Procedure of digitalization: To physically identify X-ray films, we employ a negatoscope with a professional camera in a darkroom setting. The X-ray films were positioned on the negatoscope and photographed from a distance of 200 mm, separating the camera projector and the negatoscope.

Upon capturing images of all X-ray films, we download the digital files and systematically number them following the physical X-ray films' identification.

3) Labeling: The labeling phase is carried out by qualified individuals possessing the following credentials: NDT certification from the American Society for Non-Destructive Testing (ASNT) at level II in radiography testing and the designation of International Welding Technologist.

V. Simulation and Results

A. Training procedure

As we can figure out in Figure 14, we have two YOLO models for detecting the welding zone and the detection and recognition of the discontinuities in the welding zone.

Table III highlights the information related to the film training process. The images contain many welding types and positions and different quality image levels.

TABLE III: Training film procedure information

		Training	Validation
Welding detection	*Number of images*	1016	180
	Image size	640x640	640x640
Welding discontinuities	*Number of images*	790	80
	Image size	640x640	640x640

Models used in our approach are mixed between different YOLO-v5 [31] and yolo6 [32] (table IV), with training hyperparameters as follows:

- Image size: 640x640
- Optimizer: Stochastic gradient descent
- Batch size: 16

TABLE IV: Models used in welding detection and welding discontinuities

	Name	Weights
Detection	*YOLOv5s*	7.2 Millions
	YOLOv5m	21.2 Milions
	YOLOv6s	18.5 Milions
	YOLOv6m	34.9 Milions
Discontinuities	*YOLOv5l*	46.5 Milions
	YOLOv5x	86.7 Milions
	YOLOv6l	59.6 Milions
	YOLOv6l6	140.4 Milions

B. Results and evaluations

The proposed training processes mentioned above exhibit consistent welding and discontinuity detection convergence across various models. This convergence highlights the effectiveness and reliability of these methods in tackling the specific challenges of weld analysis and defect detection.

However, there are significant differences in terms of convergence speed and accuracy among each model. These differences exist not only within the same architecture but also between closed-size models.

1) Welding zone detection model: Comparing the YOLO 5 outcomes, the results depicted in Figures 15a and 15b reveal comparable performance in class loss minimization between the small (YOLOv5s) and medium (YOLOv5m) weight models. However, a nuanced disparity emerges, highlighting a favorable edge for the medium model in box loss minimization. For YOLOv6 outcomes concerning the detection of welding zones, it is evident from Figures 16a and 16b that the medium model exhibits a slight advantage in class and box loss compared to its smaller one. Nevertheless, Figure 17b and Figure 17b manifest the prevalence of the YOLOv5 model over YOLOv6 concerning loss values during the training process for welding zone detection.

For the precision context, there is, as shown in Figures 18a,18b,19a and 19b, a good performance of the medium models of YOLOv5 and YOLOv6 compared to the small ones. This gap between the two weight size models becomes highlighted in the mean average precision mAP-50-95. However, comparing the two architectures, YOLOv5

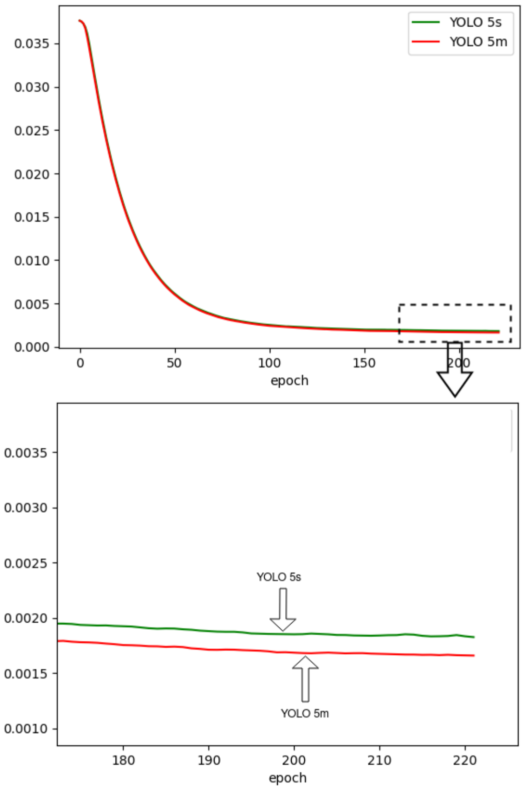

(a) Loss of classes

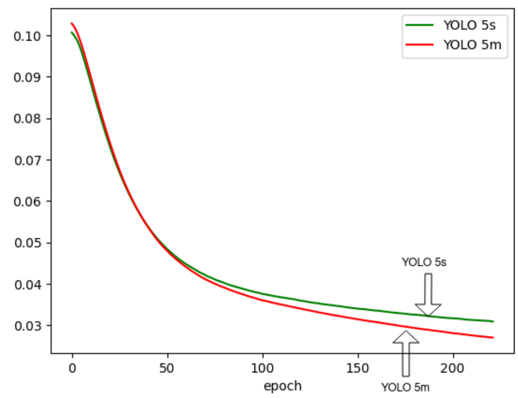

(b) Loss of box

Fig. 15: Losses of YOLOv5s and YOLOv5m in the training stage for welding detection

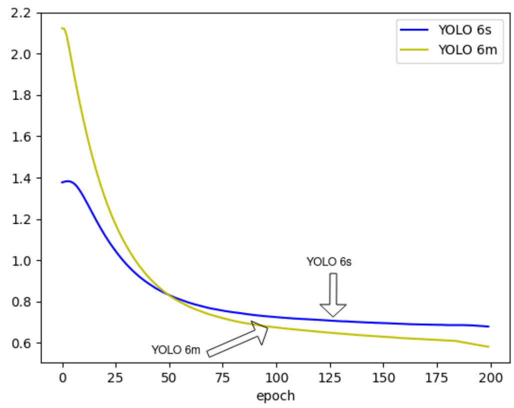

(a) Loss of classes

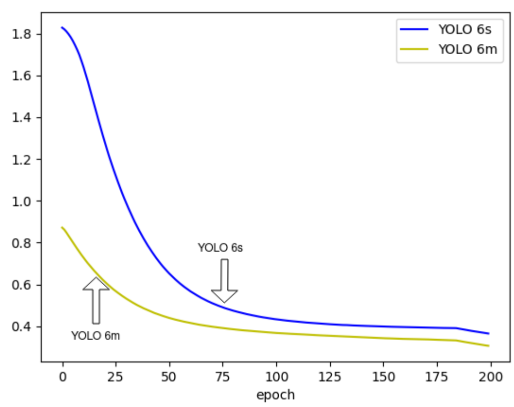

(b) Loss of box

Fig. 16: Losses of YOLOv6s and YOLOv6m in the training stage for welding detection

outperforms YOLO6, as figured out in Figures 20a and 20b.

2) Welding discontinuity detection model: For discontinuity detection, as a complex task, compared to welding zone detection, we can see a slow convergence of the loss function for both the YOLOv5 and YOLOv6 models (Figures 21a, 21b, 22a and 22b). Nonetheless, the results shown in Figures 23a, 23b reveal a gap in loss values between the two versions of YOLO, which is an advantage to YOLOv5.

The precision analysis depicts, in fact, the good performance of YOLOv6 models in discontinuity detection compared to YOLOv5 models, as shown in Figures 26a and 26b. In fact, there is a slow evolution of precision values within the training epochs in the YOLOv5 models (Figures 24a and 24b). On the contrary, YOLOv6 models present good precision evolution within training epochs, as shown in Figures 25a and 25b.

C. Inference

In order to assess the pragmatic applicability of the proposed model within real-world scenarios, the inference results, encompassing the progression from the raw target image to the identification of weld discontinuities will be

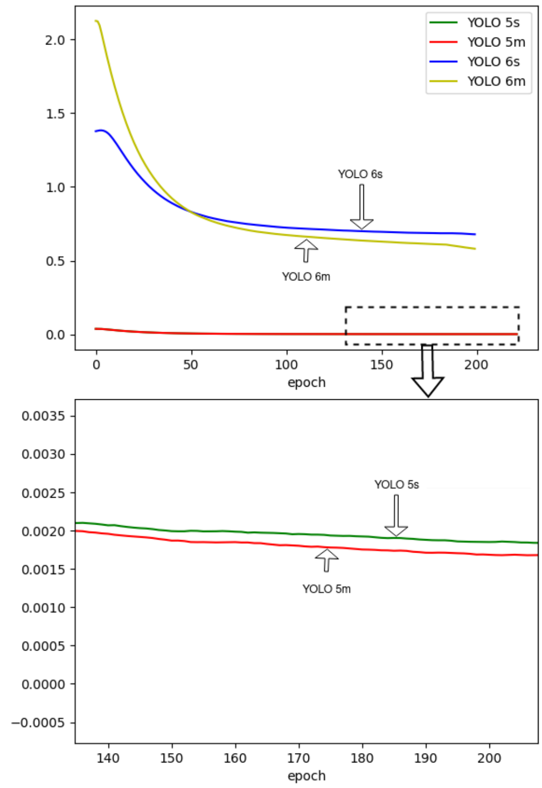

(a) Loss of classes

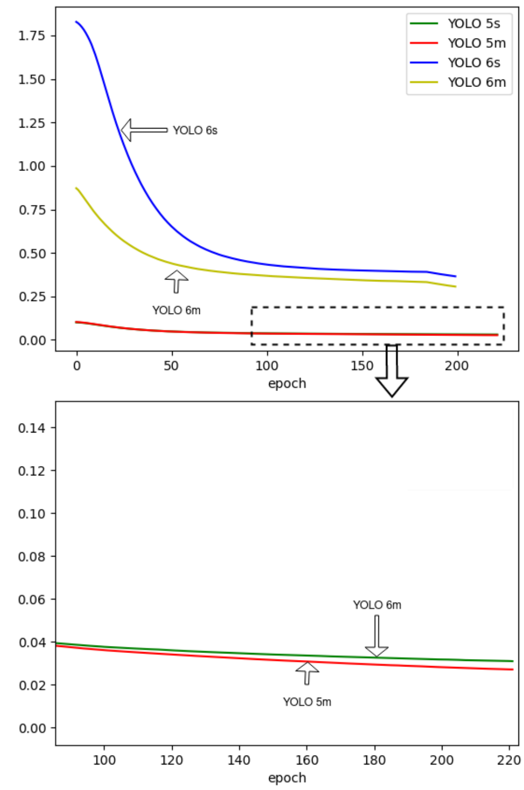

(b) Loss of box

Fig. 17: Losses of YOLOv5 and YOLOv6 models in the training stage for welding detection

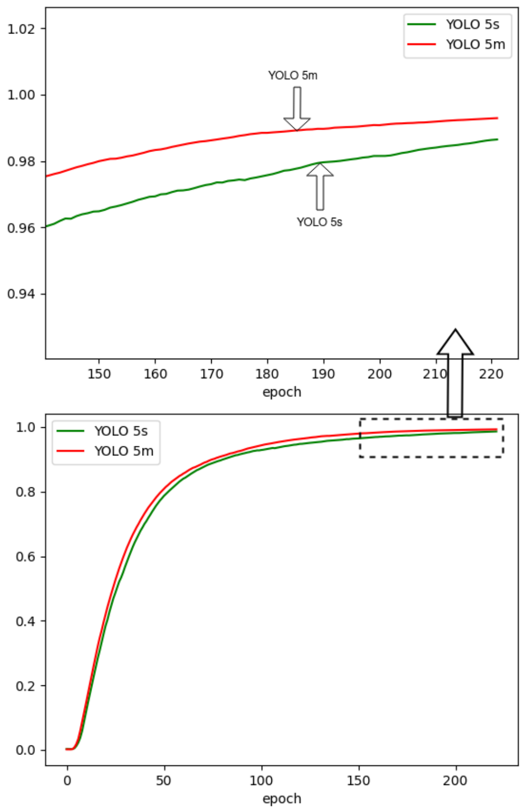

(a) mAP-0%:50%

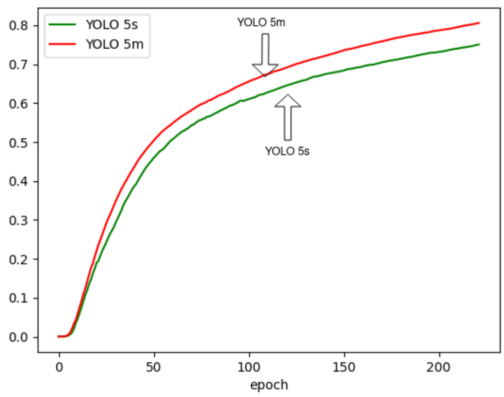

(b) mAP-50%:95%

Fig. 18: Mean Average Precision (mAP) of YOLOv5 models in the training stage for welding detection

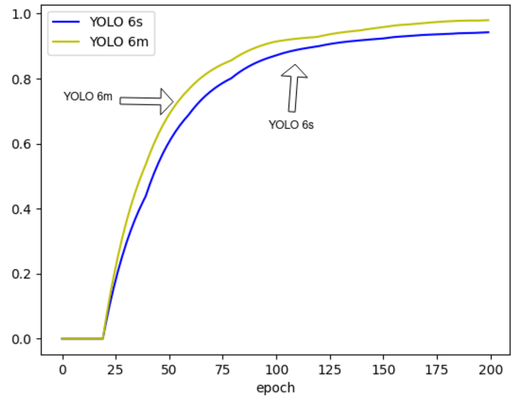

(a) mAP-0%:50%

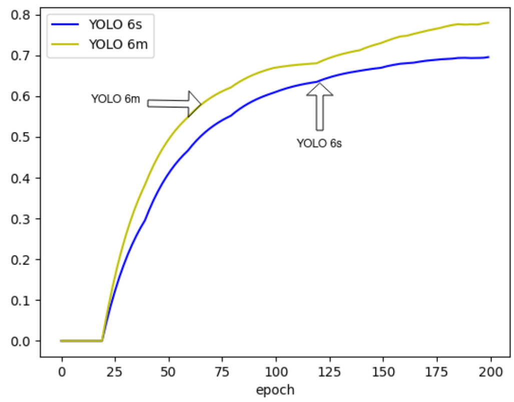

(b) mAP-50%:95%

Fig. 19: Mean Average Precision (mAP) of YOLOv6 models in the training stage for welding detection

examined.

Tables V and VI highlight the inference results derived from various instances of weld radiographs. The evaluated images exhibit good performance in detection scenarios for both Yolo 5 and Yolo 6 models. Notably, in the context of discontinuity detection, Yolo 5 models demonstrate superior results when compared to their Yolo 6 counterparts.

TABLE V: Examples of welding radiographs inference results using Yolo detection models.

Yolo 5s

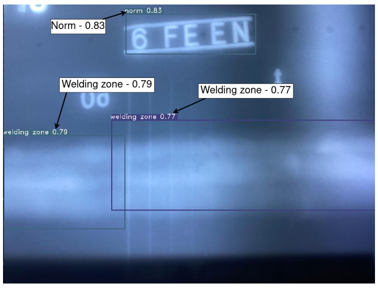

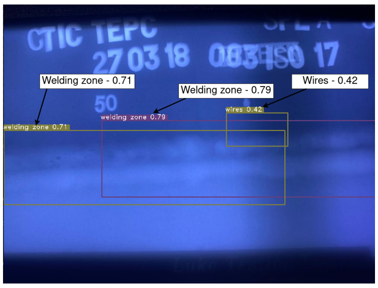

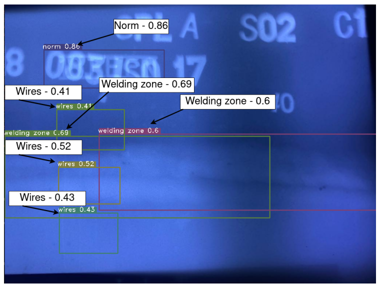

Yolo 5m

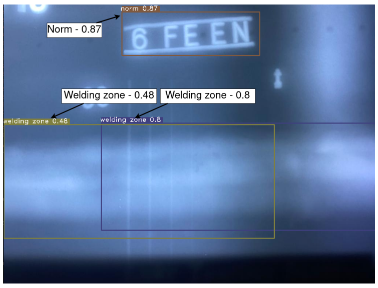

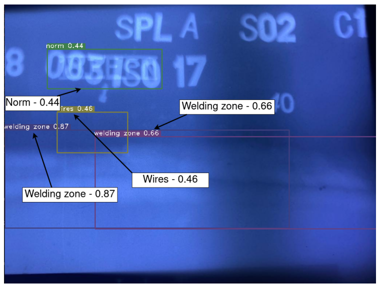

Yolo 6s

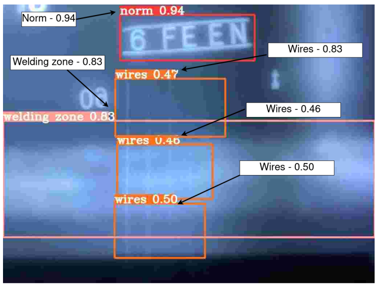

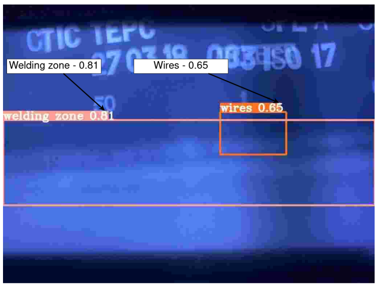

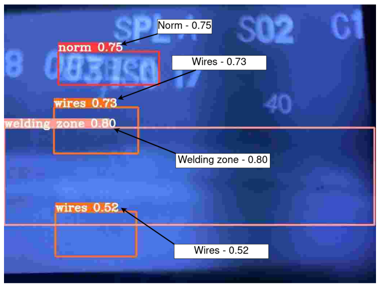

Yolo 6m

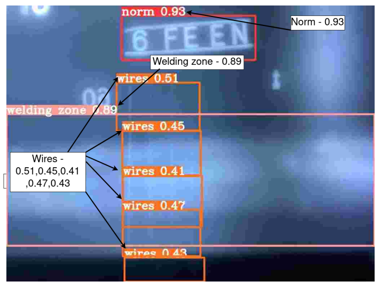

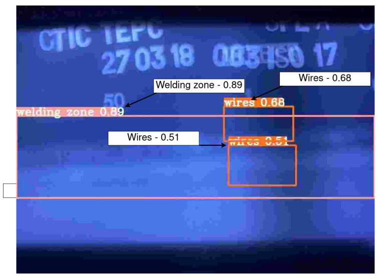

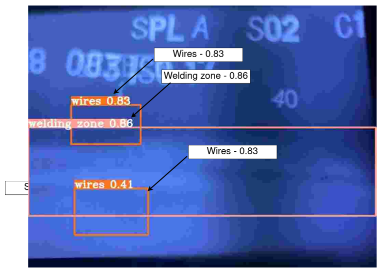

TABLE VI: Examples of welding radiographs inference results using Yolo discontinuities models.

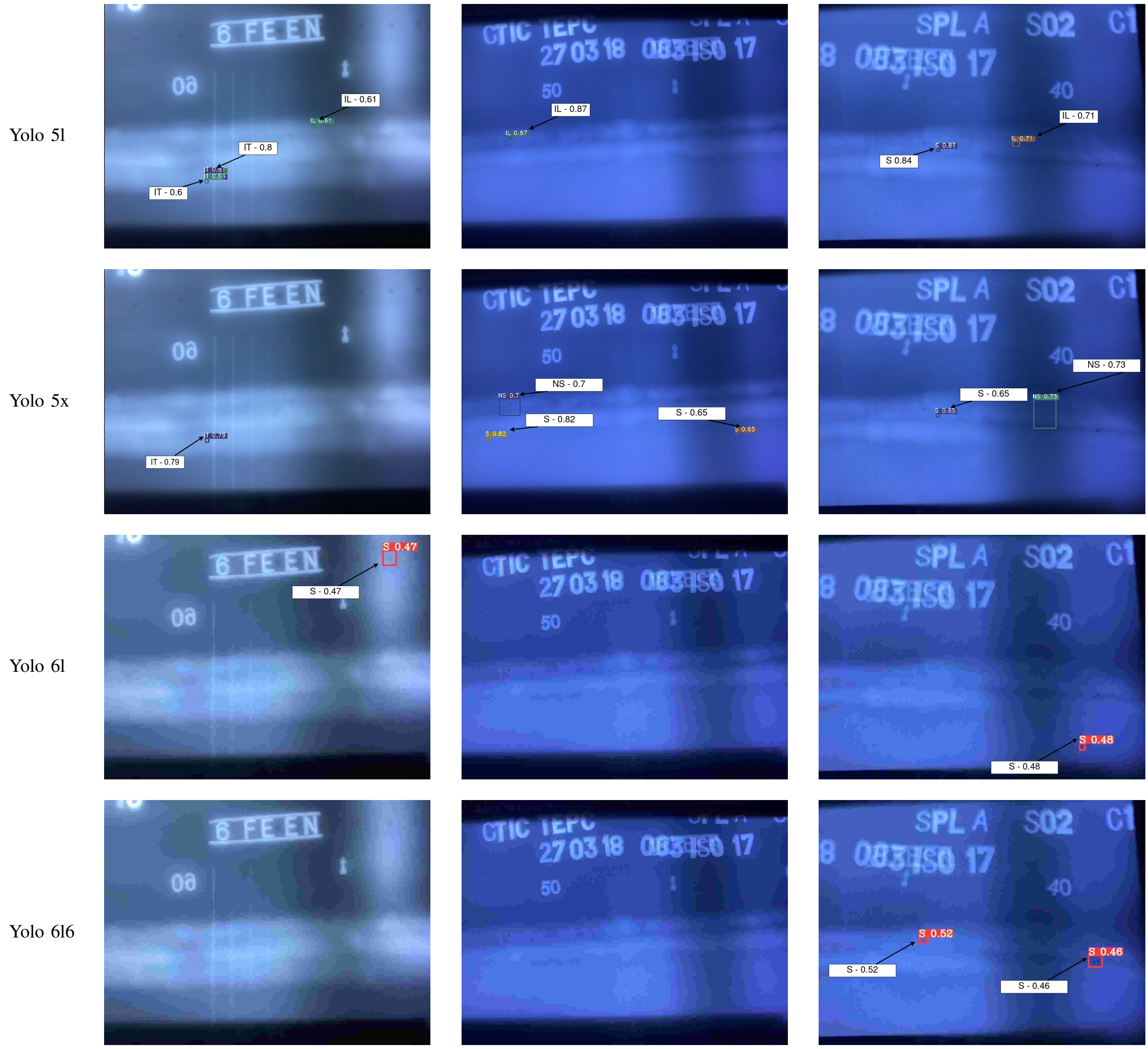

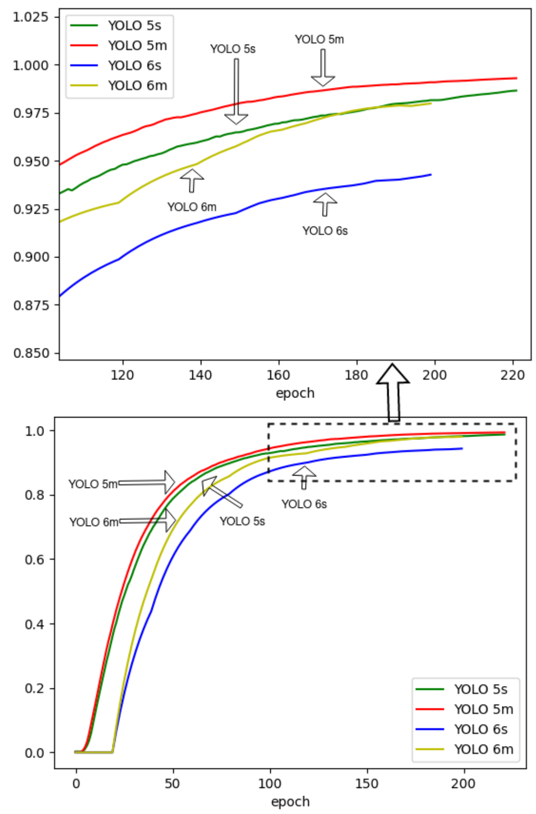

(a) mAP-0%:50%

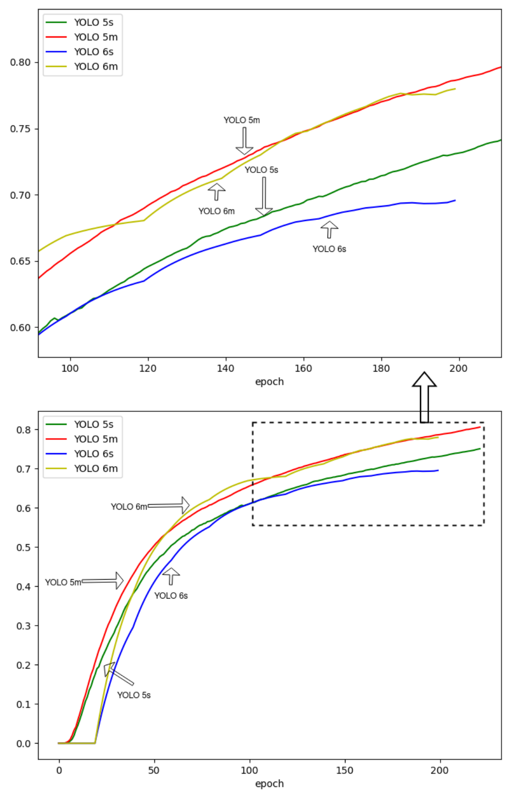

(b) mAP-50%:95%

Fig. 20: Mean Average Precision (mAP) of all models in the training stage for welding detection

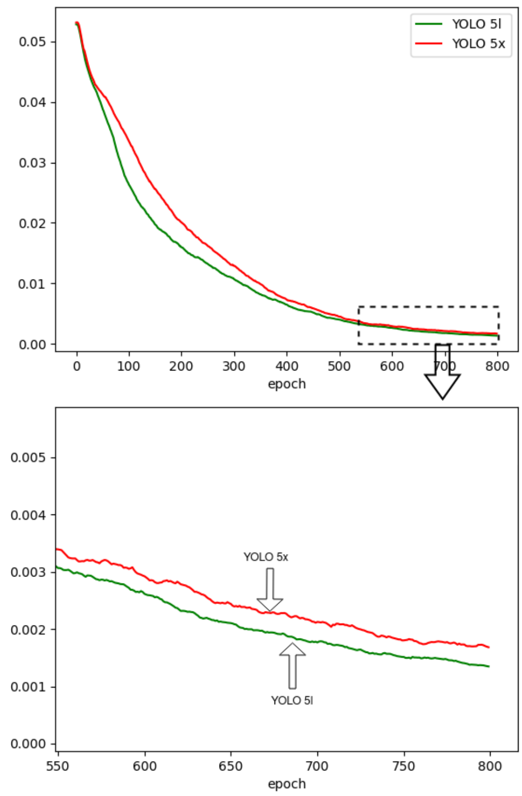

(a) Loss of classes

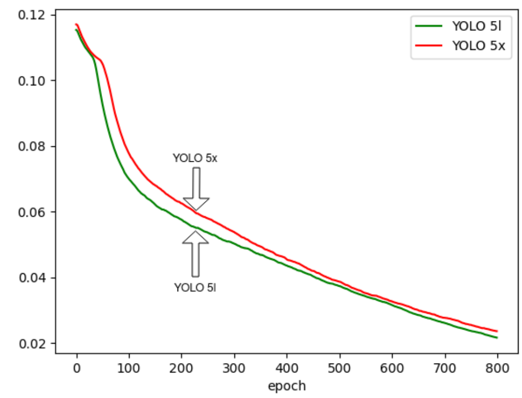

(b) Loss of box

Fig. 21: Losses of YOLOv5l and YOLOv5x in the training stage for welding discontinuity detection

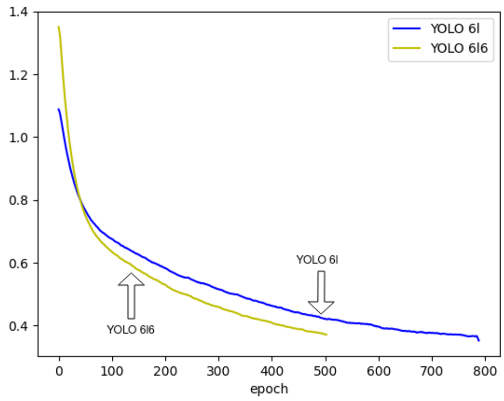

(a) Loss of classes

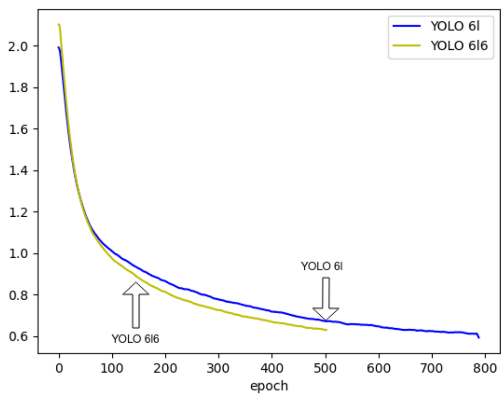

(b) Loss of boxes

Fig. 22: Losses of YOLOv6l and YOLOv6l6 in the training stage for welding discontinuity detection

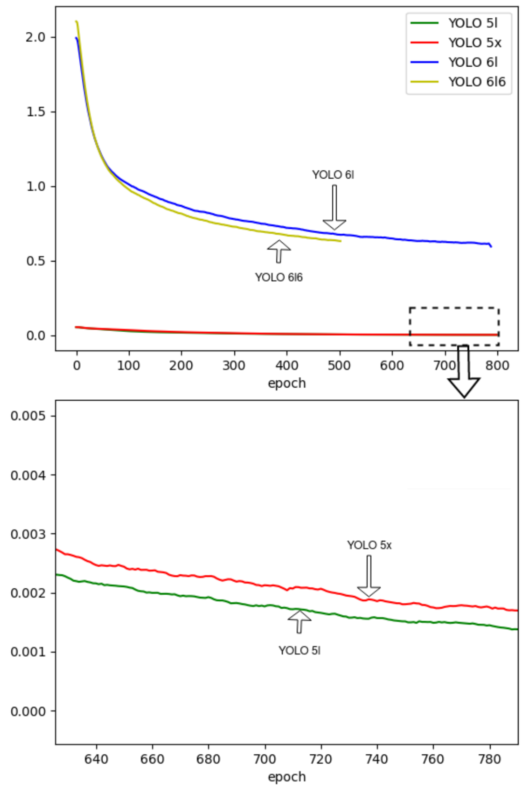

(a) Loss of classes

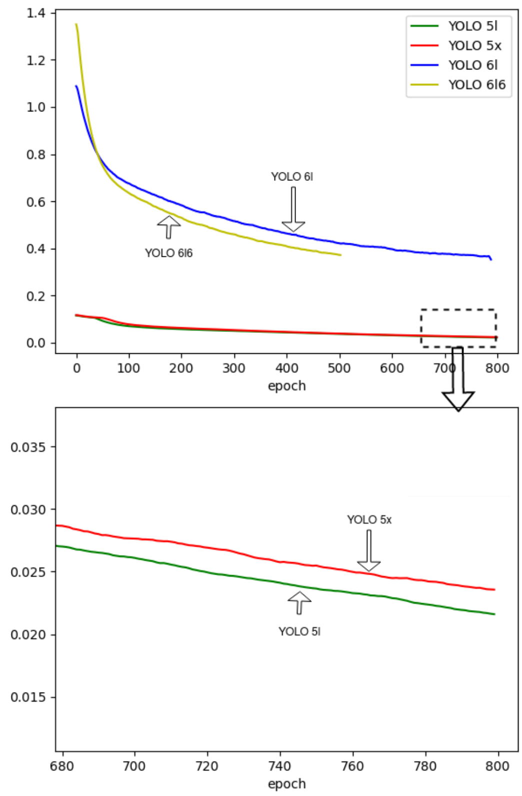

(b) Loss of boxes

Fig. 23: Losses of YOLOv5 and YOLOv6 models in the training stage for welding discontinuity detection

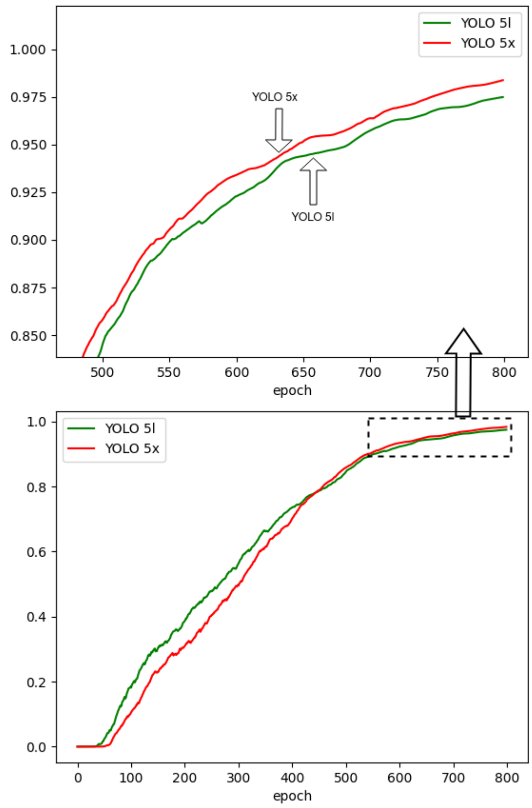

(a) mAP-0%:50%

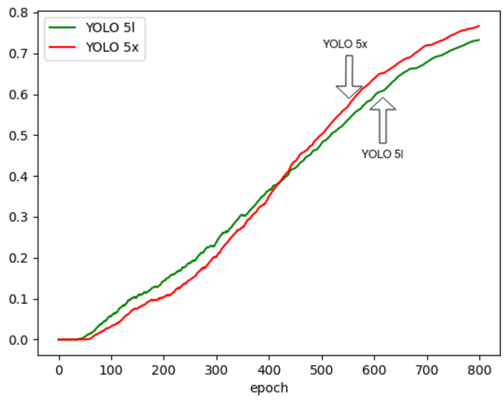

(b) mAP-50%:95%

Fig. 24: Mean Average Precision (mAP) of YOLOv5 models in the training stage for welding discontinuity detection

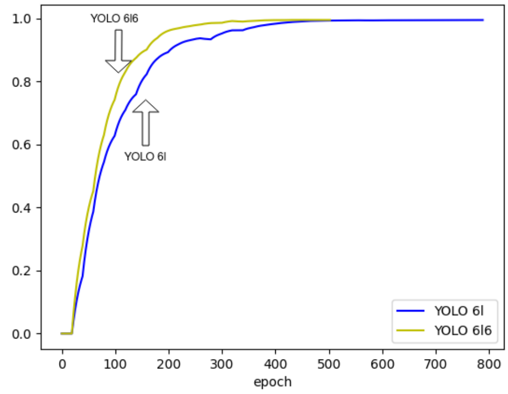

(a) mAP-0%:50%

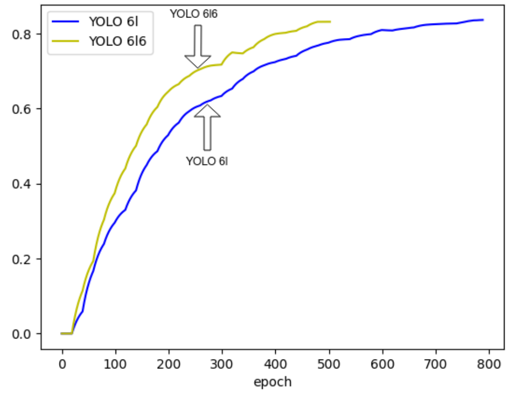

(b) mAP-50%:95%

Fig. 25: Mean Average Precision (mAP) of YOLOv6 models in the training stage for welding discontinuity detection

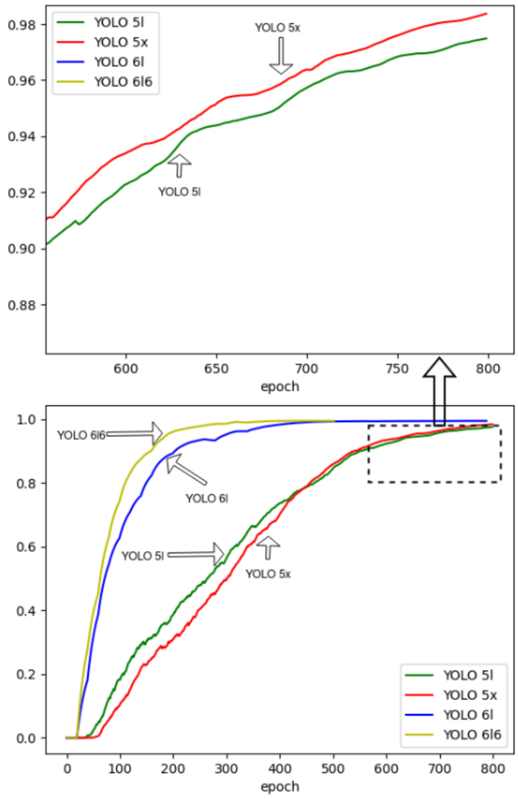

(a) mAP-0%:50%

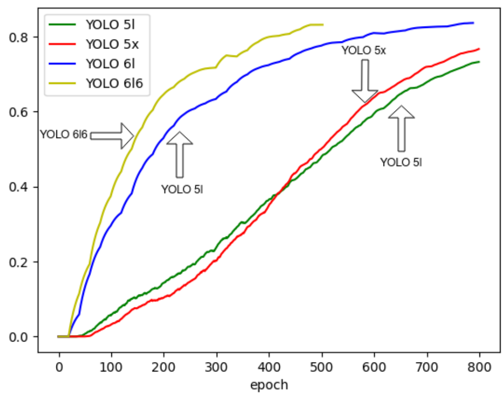

(b) mAP-50%:95%

Fig. 26: Mean Average Precision (mAP) of all models in the training stage for welding discontinuity detection

VI. Conclusion

In this paper, a turn-key system is presented. It offers automatic detection of welding zones and film quality, along with the classification of discontinuities in weld process piping assembly. This system is designed with high generalization capabilities that extend beyond specific industry or piping size requirements.

With the advent of technological evolution in radiographic control, the field of digital radiography usage can be expanded. Our proposed solution, which digitizes numerical X-ray film, offers an opportunity for its widespread use.

It is important to note that while our proposed solution cannot fully replace human interpretation, it can complement it by making the interpretation task more manageable.

In conclusion, this turn-key system represents an important advancement in the welding industry, with the potential to revolutionize welding quality evaluation and maintenance practices.

References

[1] Markets & Markets. 2019. Industrial tubes market: forecast to 2023. https://www.marketsandmarkets.com/Market-Reports/industrial-tube-market- 3455514.html

[2] Lakhani, Paras, and Baskaran Sundaram. "Deep learning at chest radiography: automated classification of pulmonary tuberculosis by using convolutional neural networks." Radiology 284.2 (2017): 574-582.

[3] Erickson, Bradley J., et al. "Machine learning for medical imaging." Radiographics 37.2 (2017): 505.

[4] Markets & Markets. 2021. Image recognition market: forecast to 2025. https://www.marketsandmarkets.com/Market-Reports/image-recognition-market- 222404611.html

[5] Mirapeix, J., et al. "Real-time arc-welding defect detection and classification with principal component analysis and artificial neural networks." NDT & e International 40.4 (2007): 315-323.

[6] O'Mahony, Niall, et al. "Deep learning vs. traditional computer vision." Science and information conference. Springer, Cham, 2019.

[7] Hou, Wenhui, et al. "Review on computer aided weld defect detection from radiography images." Applied Sciences 10.5 (2020): 1878.

[8] Golodov, V. A., and A. A. Maltseva. "Approach to weld segmentation and defect classification in radiographic images of pipe welds." NDT & E International 127 (2022): 102597.

[9] Hou, Wenhui, et al. "Deep features based on a DCNN model for classifying imbalanced weld flaw types." Measurement 131 (2019): 482-489.

[10] Piping, Process. "ASME B31. 3." The American Society of Mechanical Engineers: New York, NY, USA (2010).

[11] Lohmeier, Alfred, Richard E. Deremiah, and Louis E. Hayden Jr. "Part A: Piping Fundamentals."

[12] Boiler, A. S. M. E., and Pressure Vessel Code. "Section V." Nondestructive examination (2010).

[13] Zscherpel, U., et al. "Neue Entwicklungen bei der Filmdigitalisierung." DGZfP-Jahrestagung in Aachen, Tagungsband (1995)..

[14] Strang, Gilbert. "Wavelets and dilation equations: A brief introduction." SIAM review 31.4 (1989): 614-627.

[15] Wang, Gang, and T. Warren Liao. "Automatic identification of different types of welding defects in radiographic images." Ndt & E International 35.8 (2002): 519-528.

[16] Li, Lixin, et al. "Welding quality monitoring of high frequency straight seam pipe based on image feature." Journal of Materials Processing Technology 246 (2017): 285-290.

[17] Zapata, Juan, Rafael Vilar, and Ramón Ruiz. "Performance evaluation of an automatic inspection system of weld defects in radiographic images based on neuro-classifiers." Expert Systems with Applications 38.7 (2011): 8812-8824.

[18] El-Tokhy, Mohamed S., and Imbaby I. Mahmoud. "Classification of welding flaws in gamma radiography images based on multi-scale wavelet packet feature extraction using support vector machine." Journal of Nondestructive Evaluation 34.4 (2015): 1-17.

[19] Shafeek, H. I., et al. "Assessment of welding defects for gas pipeline radiographs using computer vision." NDT & e International 37.4 (2004): 291-299.

[20] Ye, Han, et al. "Detection and recognition of defects in X-ray images of welding seams under compressed sensing." Journal of Physics: Conference Series. Vol. 1314. No. 1. IOP Publishing, 2019.

[21] Redmon, Joseph, et al. "You only look once: Unified, real-time object detection." Proceedings of the IEEE conference on computer vision and pattern recognition. 2016.

[22] Liu, Wei, et al. "Ssd: Single shot multibox detector." European conference on computer vision. Springer, Cham, 2016.

[23] Lin, Tsung-Yi, et al. "Focal loss for dense object detection." Proceedings of the IEEE international conference on computer vision. 2017.

[24] Zhang, Haoyang, et al. "Varifocalnet: An iou-aware dense object detector." Proceedings of the IEEE/CVF Conference on Computer Vision and Pattern Recognition. 2021.

[25] Yang, Ze, et al. "Reppoints: Point set representation for object detection." Proceedings of the IEEE/CVF International Conference on Computer Vision. 2019.

[26] Gavrilescu, Raducu, et al. "Faster R-CNN: an approach to real-time object detection." 2018 International Conference and Exposition on Electrical And Power Engineering (EPE). IEEE, 2018.
[27] Cai, Zhaowei, and Nuno Vasconcelos. "Cascade r-cnn: Delving into high quality object detection." Proceedings of the IEEE conference on computer vision and pattern recognition. 2018.
[28] Dai, Jifeng, et al. "R-fcn: Object detection via region-based fully convolutional networks." Advances in neural information processing systems 29 (2016).
[29] Zhang, Hongkai, et al. "Dynamic R-CNN: Towards high quality object detection via dynamic training." European conference on computer vision. Springer, Cham, 2020.
[30] Reza, Ali M. "Realization of the contrast limited adaptive histogram equalization (CLAHE) for real-time image enhancement." Journal of VLSI signal processing systems for signal, image and video technology 38.1 (2004): 35-44.
[31] Glenn, Jocher, et al."ultralytics/yolov5: v5.0 - YOLOv5-P6 1280 models, AWS, Supervise.ly and YouTube integrations" Zenodo, 2022
[32] Li, Chuyi, et al. "YOLOv6: A single-stage object detection framework for industrial applications." arXiv preprint arXiv:2209.02976 (2022).

Adil EL HARRAK is a mechanical and structural engineer from ENSAM, Moulay Ismail University, Meknes, since 2010 in Morocco. He is an International Welding Technologist (IWT) since 2014 from the International Institute of Welding (IIW) and a certified ASNT NDT level II since 2020. With more than 12 years of experience in the fields of materials science, metallurgy, and welding. He is currently working as a piping and structure consultant with oil and gas subcontractors. https://orcid.org/0009-0004-1181-6539

Mohamed RHAZZAF (M'270493) is currently working as an assistant professor and researcher in computer science and artificial intelligence at the Euro-Mediterranean University of Fes, Fes, Morocco. He received an engineering degree in computer science from the Mohammadia School of Engineering EMI, Mohammed V University Rabat, Morocco, in 2011. He had a Ph.D. in artificial intelligence and machine learning at the Doctoral Studies Center at ENSAM, Moulay Ismail University, Meknes, Morocco, in 2020. He is a member of the Laboratory of Mathematical Modeling, Simulation, and Smart Systems (L2M3S) and of the Artificial Intelligence for Engineering Sciences Team (IASI) at ENSAM. His research interests include artificial intelligence, machine learning, deep learning, swarm intelligence, and numerical optimization. https://orcid.org/0000-0002-2330-7465.

Imane MOUMENE is graduated in 2019 as an industrial and production engineer from ENSAM, University Moulay Ismail, Meknes, Morocco. She is actually an inspection (NDT & Lifting) manager with several certificates in NDT as level II: PAUT, UT, MT, LPT, and RT lifting.